IEEE Photonics Journal
An IEEE Photonics Society Publication

Open Access

Photonic Generation of Radio-Frequency Waveforms Based on Dual-Parallel Mach–Zehnder Modulator

Volume 6, Number 3, June 2014

Wei Li, Member, IEEE
Wen Ting Wang
Ning Hua Zhu, Member, IEEE

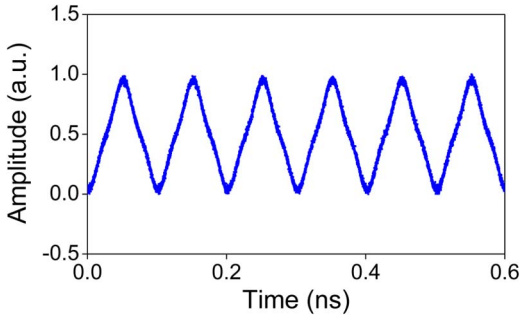

DOI: 10.1109/JPHOT.2014.2325863
1943-0655 © 2014 IEEE

IEEE photonics SOCIETY

IEEE

Photonic Generation of Radio-Frequency Waveforms Based on Dual-Parallel Mach–Zehnder Modulator

Wei Li, *Member, IEEE*, Wen Ting Wang, and Ning Hua Zhu, *Member, IEEE*

State Key Laboratory on Integrated Optoelectronics, Institute of Semiconductors, Chinese Academy of Sciences, Beijing 100083, China

DOI: 10.1109/JPHOT.2014.2325863

Manuscript received April 17, 2014; accepted May 14, 2014. Date of publication May 20, 2014; date of current version May 30, 2014. This work was supported by the National Natural Science Foundation of China under 61377069, 61335005, 61108002, 61321063, and 61090391. Corresponding author: N. H. Zhu (e-mail: nhzhu@semi.ac.cn).

Abstract: We report a photonic approach to generating radio-frequency (RF) waveforms based on a dual-parallel Mach–Zehnder modulator (DPMZM) driven by a sinusoidal RF signal. One of the sub-MZMs (MZM1) of the DPMZM is driven by the sinusoidal RF signal, whereas the other sub-MZM (MZM2) has no driven signal. In this way, the powers of even- and odd-order sidebands can be separately controlled by adjusting the bias of the MZM1. The power ratio between the odd- (or even-) order sidebands is tunable by adjusting the RF power. Moreover, the power and the phase of the optical carrier can be independently tunable by adjusting the biases of the MZM2 and the parent MZM of the DPMZM, respectively. After detecting by a photodetector, an RF signal with controllable harmonics is generated. Thus, a desired RF waveform can be generated by separately manipulating its harmonics. The proposed method is theoretically analyzed. In addition, proof-of-concept experiments are carried out to generate triangular and rectangular waveforms with repetition rates of 5 and 10 GHz.

Index Terms: Radio-frequency waveform generation, dual-parallel Mach–Zehnder modulator.

1. Introduction

Generation of arbitrary radio-frequency (RF) waveforms has attracted great attentions in recent years due to its widespread applications such as RF signal processing, optical analog and digital communications, wireless communications, and radar [1]–[7]. Due to the limited sampling rate, the generation of RF waveform in the electrical domain is limited to a low frequency and small bandwidth [1]. On the other hand, photonic generation of RF waveforms benefits from the advantages brought by the microwave photonics techniques, e.g. wide bandwidth, low loss (using optical fiber), and immunity to electromagnetic interference. Photonic generation of RF waveform can be realized using Fourier synthesis method [8]. An optical frequency comb generated by a mode locked laser is tailored by an optical spectral shaper. The desired RF waveform can be obtained by detecting the tailored optical signal in a photodetector (PD) [9]. Furthermore, arbitrary RF waveform can also be generated based on frequency-to-time mapping [1], [10]. The optical spectrum of an optical frequency comb is preprogrammed to be a scaled version of the desired RF waveform. After frequency-to-time mapping via a dispersive element, the desired RF waveform is generated in the PD.

RF waveform generation has also been proposed using external modulation of a continuous wave (CW) optical signal [11]–[16]. A series of optical sidebands are generated due to the nonlinearity of the external modulator. The desired RF waveforms are generated by controlling the phases and amplitudes of the optical sidebands. It was reported that triangular waveform can be generated using a Mach–Zehnder modulator (MZM) in conjunction with an optical interleaver [11] or a dispersive element [12]. The structure based on the MZM and optical interleaver suffers from the stability problem due to the use of Mach–Zehnder interferometer. In [12], the repetition rate of the generated waveform is fixed for a given length of dispersive fiber. Recently, Liu *et al.* reported a method to generating triangular waveforms using a MZM biased at the null point and stimulated Brillouin scattering (SBS) in optical fiber [13]. However, the SBS effect is sensitive to the environmental fluctuations, which may make the system unstable. In [14], [15], triangular waveforms were generated using a DPMZM in conjunction with a frequency tripler or a 90° electrical hybrid coupler. It is noted that the schemes reported in [11]–[15] are particularly designed to generate triangular waveforms. They might not be able to generate other types of RF waveforms. For generation of versatile RF waveforms, a method using a polarization modulator (PolM) inserted in a Sagnac loop was proposed in [16]. The bidirectional use of the PolM generates an intensity-modulated optical signal plus an unmodulated optical carrier. By properly controlling the polarization controllers, the power of the optical carrier, the even-, and odd-order sidebands can be separately controlled. As a result, the desired RF waveform can be generated by separately manipulating its harmonics. However, it may suffer from the stability problem due to the use of Sagnac interferometer loop.

In this paper, a new photonic approach to generating RF waveforms based on a DPMZM is proposed. Different from other schemes based on DPMZM [14], [15], we can generate not only triangular waveform but also other waveforms. Moreover, the sinusoidal RF signal is only driven to one of the sub-MZM (MZM1) of the DPMZM, while the other sub-MZM (MZM2) has no driven signal. Thus, a frequency multiplier or a 90° electrical hybrid coupler used in [14], [15] are no longer required in our approach. It is noted that the RF waveforms generated using optical comb and optical spectra shaping or filtering [10] usually have small duty cycle. However, our approach is capable of generating RF waveforms with a full duty cycle. In our scheme, the powers of the even- and odd-order optical sidebands can be separately controlled by adjusting the bias of the MZM1. The power ratio between the odd- (or even-) order sidebands can be adjusted by tuning the RF power. Furthermore, the power and the phase of the optical carrier can be independently tuned by adjusting the biases of the MZM2 and the parent MZM of the DPMZM. After detecting in a PD, an RF signal with controllable harmonics is generated. In this way, a desired RF waveform with a full-duty-cycle can be generated by separately manipulating its harmonics. Actually, the method of manipulating the optical sidebands used in our scheme is similar to that in [16]. However, the key significance of our approach is that we use a compact structure of DPMZM which is expected to be more stable than the Sagnac loop based system [16]. The proposed method is theoretically analyzed. In addition, proof-of-concept experiments are carried out to generate triangular and rectangular waveforms with repetition rates of 5 and 10 GHz.

2. Principle

The schematic diagram of the proposed RF waveforms generator is shown in Fig. 1. An optical carrier from a laser diode (LD) is sent to a DPMZM which is formed by two sub-MZMs (MZM1 and MZM2) laying on each arm of a parent MZM (MZM3). The MZM1 is driven by a sinusoidal RF signal. Thus, the optical field at the output of the MZM1 is given by

$$E_{MZM1}(t) = \frac{E_{in}(t)}{\sqrt{2}}\left[\cos\left(\beta \sin \omega_{rf} t + \frac{\varphi_1}{2}\right)\right] \tag{1}$$

where $E_{\text{in}}(t) = \exp(j\omega_0 t)$ is the normalized electrical field of the optical carrier, ω_0 is the angular frequency of the optical carrier, $\beta = \pi V_{\text{rf}}/V_{\pi 1}$ is the modulation index of the MZM1, V_{rf} and ω_{rf} are the amplitude and angular frequency of the MZM1, respectively, $V_{\pi 1}$ is the half-wave voltage of the MZM1, $\varphi_1 = \pi V_1/V_{\pi 1}$ is the phase shift between the two arms of the MZM1, which is controlled by

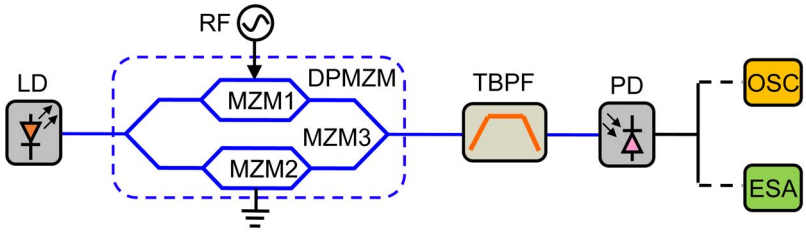

Fig. 1. Schematic diagram of the proposed RF waveforms generator (LD: laser diode; DPMZM: dual-parallel Mach–Zehnder modulator; TBPF: tunable bandpass filter; PD: photodetector, OSC: oscilloscope, ESA: electrical spectrum analyzer).

the DC bias, V_1, of the MZM1. On the other hand, the MZM2 has no RF driven signal. The optical field at the output of the MZM2 can be expressed as

$$E_{MZM2}(t) = \frac{1}{\sqrt{2}} E_{in}(t)\cos\left(\frac{\varphi_2}{2}\right) \tag{2}$$

where $\varphi_2 = \pi V_2 / V_{\pi 2}$ is the phase shift between the two arms of the MZM2, which is controlled by the DC bias, V_2, of the MZM2. $V_{\pi 2}$ is the half-wave voltage of the MZM2. At the output of the DPMZM, the optical field is given by

$$E_{DPMZM}(t) = \frac{1}{\sqrt{2}}\left[E_{MZM1}(t)\exp\left(\frac{j\varphi_3}{2}\right) + E_{MZM2}(t)\exp\left(\frac{-j\varphi_3}{2}\right)\right] \tag{3}$$

where $\varphi_3 = \pi V_3 / V_{\pi 3}$ is the phase shift between the MZM1 and MZM2, which is controlled by the DC bias, V_3, of the parent MZM3. Substituting (1) and (2) to (3) and applying Jacobi–Anger expansion to (3), we have

$$E_{DPMZM}(t) = \frac{1}{2}E_{in}(t)\sum_{n=-\infty}^{\infty}\cos\frac{\varphi_1 - n\pi}{2} J_n(\beta)\exp\left(jn\omega_{rf}t + j\frac{n\pi}{2} + \frac{j\varphi_3}{2}\right) + \frac{1}{2}E_{in}(t)\cos\left(\frac{\varphi_2}{2}\right)\exp\left(\frac{-j\varphi_3}{2}\right). \tag{4}$$

The optical signal consists of an optical carrier and a series of sidebands. The negative sidebands are related to the lower frequency shifts by the optical carrier, while the positive sidebands are related to the upper frequency shifts by the optical carrier. The phase of the optical carrier is tunable by adjusting the DC bias, V_3, of the parent MZM3. This point is very important for our scheme to generate the desired RF waveform. As can be seen from (4), the negative and positive sidebands are out of phase. If this optical signal is detected by a photodetector (PD), the powers of the generated RF signals vary with the DC bias, V_3, of the parent MZM3. For example, the fundamental RF signal cannot be detected if the phase of the optical carrier is tuned to be $-\pi/2$ because the beating signal between the first-order positive sideband (with phase of $\pi/2$) and the optical carrier will cancel that between the optical carrier and the first-order negative sideband (with phase of $-\pi/2$) out perfectly. In order to overcome this limitation, a tunable bandpass filter (TBPF) is attached after the DPMZM to remove all the negative sidebands (or the positive sidebands). It is noted that similar optical filtering technique was also used in [13], [16]. The resulted optical field at the output of the TBPF is given by

$$E_{out}(t) = \frac{1}{2}E_{in}(t)\left[\cos\left(\frac{\varphi_2}{2}\right)\exp\left(\frac{-j\varphi_3}{2}\right) + \cos\frac{\varphi_1}{2}J_0(\beta)\exp\left(\frac{j\varphi_3}{2}\right)\right] + \frac{1}{2}E_{in}(t)\sum_{n=1}^{\infty}\cos\frac{\varphi_1 - n\pi}{2}J_n(\beta)\exp\left(jn\omega_{rf}t + j\frac{n\pi}{2} + \frac{j\varphi_3}{2}\right). \tag{5}$$

After detecting by a PD, the current is given by

$$i(t) \propto E_{out}(t) \cdot E_{out}^{*}(t) \approx i_{DC} + \frac{1}{2} C \cdot \sum_{n=1}^{\infty} \cos\left(\frac{\varphi_1 - n\pi}{2}\right) J_n(\beta) \cos\left(n\omega_{rf} t + \frac{n\pi + \varphi_3}{2} - \psi\right) \tag{6}$$

where

$$C = \sqrt{\cos^2\frac{\varphi_2}{2} + J_0^2(\beta)\cos^2\frac{\varphi_1}{2} + 2J_0(\beta)\cos\frac{\varphi_1}{2}\cos\frac{\varphi_2}{2}\cos\varphi_3} \tag{6a}$$

$$\psi = arc\tan\left(\frac{J_0(\beta)\cos\frac{\varphi_1}{2} - \cos\frac{\varphi_2}{2}}{J_0(\beta)\cos\frac{\varphi_1}{2} + \cos\frac{\varphi_2}{2}} \tan\frac{\varphi_3}{2}\right). \tag{6b}$$

The photocurrent consists of a DC part, a fundamental sinusoidal RF signal, and its harmonics.

2.1. Triangular Waveform Generation

It is known that a triangular waveform can be expressed by

$$h_T(t) = A_T + B_T \sum_{n=1,3,5}^{\infty} \frac{1}{n^2} \cos(n\omega t) \tag{7}$$

where A_T and B_T are constants. The triangular waveform has a series of odd-order harmonics of the fundamental sinusoidal RF signal ω. Comparing (6) with (7), the even-order harmonics in (6) have to be eliminated. This can be done by biasing the MZM1 at the minimum transmission point, i.e. $\varphi_1 = \pi$. It means that the optical signal at the output of the TBPF consists of an optical carrier from the MZM2 of the DPMZM and odd-order sidebands from the MZM1. In the PD, the beating between the optical carrier and odd-order sidebands only generates odd-order harmonics. Moreover, $J_n(\beta)/J_1(\beta) = 1/n^2$ $(n = 3, 5, 7, \ldots)$ has to be satisfied. This condition is hard to be achieved for all harmonics. However, it has been reported [12]–[15] that a limited number of harmonics is also possible to form an approximate triangular waveform. In our case, we consider harmonics up to the third-order one. Thus, we have $\beta = 1.51$ rad for $J_3(\beta)/J_1(\beta) = 1/9$.

2.2. Rectangular Waveform Generation

A rectangular waveform can be expressed by the Fourier series as

$$h_R(t) = A_R + B_R \sum_{n=1,3,5}^{\infty} \frac{1}{n} \cos(n\omega t) \tag{8}$$

where A_R and B_R are constants. Similar to the triangular waveform, the rectangular waveform only consists of odd-order harmonics. The even-order harmonics can also be suppressed by biasing the MZM1 at the minimum transmission point. If we only consider the dc, the fundamental tone, and the third-order harmonic, $J_3(\beta)/J_1(\beta) = 1/3$ has to be satisfied. Thus, the modulation index β should be 6.1 rad.

2.3. Arbitrary Waveform Generation

The Fourier series expansion of an arbitrary waveform can be expressed as

$$h_{ar}(t) = A_{ar} + B_{ar} \sum_{n=1}^{\infty} k_n \cos(n\omega t + \phi_n) \tag{9}$$

where A_{ar} and B_{ar} are constants. Comparing (9) with (6), we have

$$\frac{k_n}{k_1} = \frac{J_n(\beta)\cos\frac{\varphi_1 - n\pi}{2}}{J_1(\beta)\cos\frac{\varphi_1 - \pi}{2}}$$

$$\phi_n = \frac{n\pi + \varphi_3}{2} - \psi \tag{10}$$

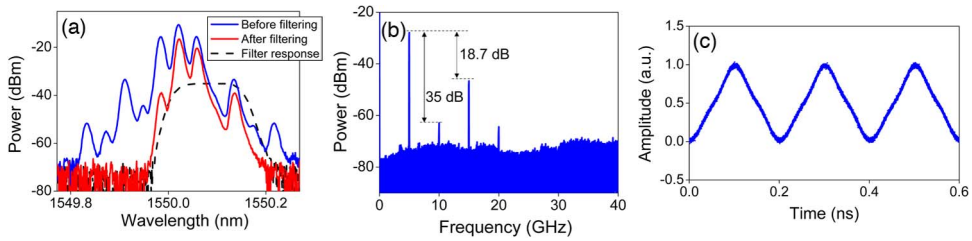

Fig. 2. Generation of 5 GHz triangular waveform. (a) The measured optical spectra before and after filtering by the TBPF. (b) The measured electrical spectrum of the 5 GHz triangular waveform. (c) The measured 5 GHz triangular waveform.

where $n = 2, 3, 4, \ldots$. For the proposed RF waveform generator, the RF harmonics up to the third-order one is controllable. Generally, the first-order, the second-order, and the third-order RF harmonics can be used to approximate most of the waveforms [16].

It is noted that the phases of the harmonics are not considered in the above analysis. We take the generation of triangular waveform as an example to show the importance of the phase information. If a time delay T_0 (T_0 can be zero) is introduced to the triangular waveform, its shape will not be changed. Thus, Eq. (7) can be rewritten as

$$h_T(t) = A_T + B_T \sum_{n=1,3,5}^{\infty} \frac{1}{n^2} \cos[n\omega(t + T_0)]. \tag{11}$$

As can be seen from Eq. (11), the phases of the harmonics have to be $n\omega T_0$ $(n = 1, 3, 5, \ldots)$. This requirement can be easily satisfied by adjusting the bias of the parent MZM, V_3.

3. Experiments

We also carried out experiments based on the experimental setup shown in Fig. 1 to verify the feasibility of the proposed RF waveform generator. An optical carrier at 1550 nm from a LD was fiber coupled to a DPMZM with a bandwidth of 20 GHz. A TBPF (Yenista XTA-50 Ultrafine) followed after the DPMZM was used to remove the lower-wavelength optical sidebands. The center wavelength (1480–1620 nm) and the bandwidth (32–650 pm) of the TBPF is tunable. The TBPF has a typical edge roll-off of 800 dB/nm and a flatness of 0.2 dB. After detecting by a PD that has a bandwidth of 40 GHz, the RF waveforms were measured using an oscilloscope (OSC) and its electrical spectra were measured using an electrical spectrum analyzer (ESA).

First, triangular waveforms were experimentally generated. A 5 GHz sinusoidal RF signal was applied to the sub-MZM (MZM1) of the DPMZM. The other sub-MZM (MZM2) of the DPMZM had no driven signal and its RF port was shorted. The half-wave voltage of the MZM1, $V_{\pi 1}$, is ~3.5 V at 5 GHz. To generate triangular waveforms, the RF power should be 17.5 dBm corresponding to the modulation index $\beta = 1.51$ rad. The bias voltages of the DPMZM was set as discussed in Section II. The measured optical spectrum at the output of the DPMZM is shown in Fig. 2(a) (blue solid line). The optical signal consists of an optical carrier and a series of sidebands. It is noted that the even-order sidebands are suppressed since the MZM1 was biased at around the minimum transmission point. After filtering by the TBPF, the optical spectrum is shown in Fig. 2(a) (red solid line). The lower-wavelength optical sidebands are removed. The undesired first-order sideband is 18.6 dB lower than the desired one. The transmission response of the TBPF is also shown in Fig. 2(a) (black dashed line). The measured electrical spectrum is shown in Fig. 2(b), which mainly consists of the fundamental tone at 5 GHz and the third-order harmonic at 15 GHz. The third-order harmonic is 18.7 dB lower than the fundamental one, which agree well with the theoretical value of 19.08 dB. Moreover, the undesired second-order harmonic RF signal is well suppressed and is 35 dB lower than the fundamental tone. The measured waveform is shown in Fig. 2(c). As can be seen, a 5 GHz triangular waveform was successfully generated.

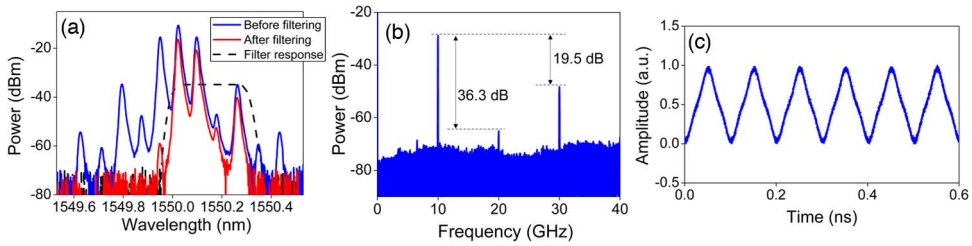

Fig. 3. Generation of 10 GHz triangular waveform. (a) The measured optical spectra before and after filtering by the TBPF. (b) The measured electrical spectrum of the 10 GHz triangular waveform. (c) The measured 10 GHz triangular waveform.

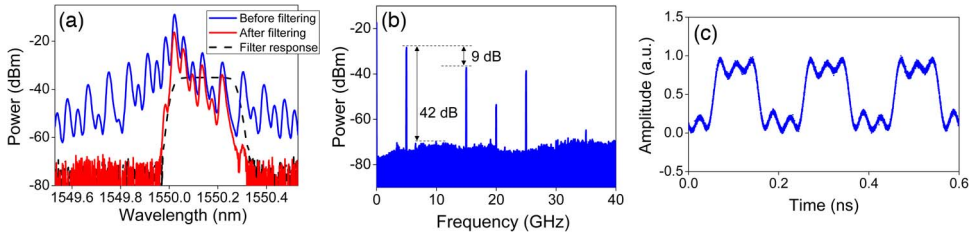

Fig. 4. Generation of 5 GHz rectangular waveform. (a) The measured optical spectra before and after filtering by the TBPF. (b) The measured electrical spectrum of the 5 GHz rectangular waveform. (c) The measured 5 GHz rectangular waveform.

In order to show the frequency tunability of the proposed RF waveform generator, the frequency of the sinusoidal RF signal applied to the MZM1 of the DPMZM was changed to 10 GHz. The measured optical spectra before and after filtering by the TBPF as well as the transmission response of the TBPF are shown in Fig. 3(a). In this case, the undesired first-order sideband is suppressed significantly and is 38 dB lower than the desired one. The measured electrical spectrum is shown in Fig. 3(b). As can be seen, the third-order harmonic at 30 GHz is 19.5 dB (close to the theoretical value of 19.08 dB) lower than the fundamental tone at 10 GHz. The second-order harmonic is suppressed and is 36.3 dB lower than the fundamental tone. The measured 10 GHz triangular waveform is shown in Fig. 3(c).

Next, we will show that the proposed RF waveform generator is also capable of generating other waveforms, e.g., RF rectangular waveform. Again, a 5 GHz sinusoidal RF signal was applied to the MZM1 of the DPMZM, while the MZM2 was shorted. In order to generate rectangular waveforms, the RF power was set to be 29.6 dBm to satisfy the requirement of $\beta = 6.1$ rad. The measured optical spectrum at the output of the DPMZM is shown in Fig. 4(a) (blue solid line). It can be seen that the even-order sidebands are properly suppressed by biasing the MZM1 at around the minimum transmission point. After filtering using the TBPF, the lower-wavelength optical sidebands are removed as shown in Fig. 4(a) (red solid line). The transmission response of the TBPF is also shown in Fig. 4(a) (black dashed line). The measured electrical spectrum is shown in Fig. 4(b). The undesired second-order harmonic is 42 dB lower than the fundamental tone. Thus, the contribution of the second-order harmonic can be ignored. The desired third-order harmonic is 9 dB lower than the fundamental tone. This value is very close to the theoretical one of 9.54 dB. The measured waveform is shown in Fig. 4(c). It can be seen that a rectangular waveform with repetition rate identical to the frequency of the reference RF signal was successfully generated.

The tunability of the repetition rate was also evaluated for the generation of rectangular waveforms. In this case, the frequency of the sinusoidal RF signal was changed to 10 GHz. The measured optical spectra before and after filtering by the TBPF as well as the transmission response of the TBPF are shown in Fig. 5(a). The resulted electrical spectrum after detecting by the PD is shown in Fig. 5(b). The electrical signal mainly consists of the fundamental tone at 10 GHz

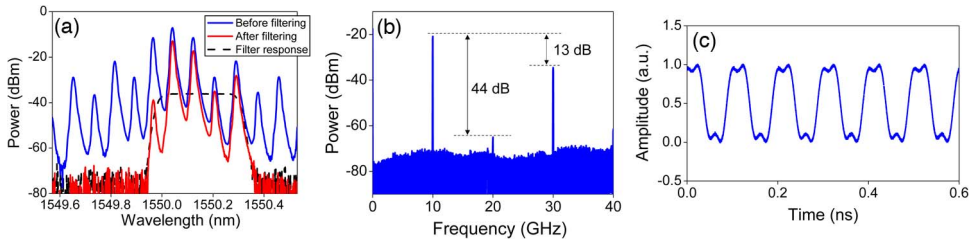

Fig. 5. Generation of 10 GHz rectangular waveform. (a) The measured optical spectra before and after filtering by the TBPF. (b) The measured electrical spectrum of the 10 GHz rectangular waveform. (c) The measured 10 GHz rectangular waveform.

and the third-order harmonic at 30 GHz. The second-order harmonic at 20 GHz can be ignored since it is 44 dB lower than the fundamental tone. The measured waveform is shown in Fig. 5(c). As can be seen, a rectangular waveform with repetition rate of 10 GHz was successfully generated.

4. Conclusion and Discussion

We have demonstrated a photonic RF waveform generator based on a DPMZM driven by a sinusoidal RF signal. The desired RF waveform can be generated by separately controlling the powers of the even- and odd-order sidebands, the power ratio between the even- (or odd-) order sidebands, and the power/phase of the optical carrier. As a result, it is possible for us to manipulate the powers of the RF harmonics after photodetecting by the PD. In this way, the desired RF waveforms can be generated. We have experimentally generated triangular and rectangular waveforms with repetition rates of 5 and 10 GHz. The generated RF waveforms are sensitive to the wavelength fluctuation of the optical carrier because the wavelength of the optical carrier has to match the transmission response of the TBPF in order to efficiently remove the undesired optical sidebands. It should be noted that the repetition rate of the generated RF waveforms is limited by the bandwidths of the DPMZM and PD. For example, the DPMZM and PD with bandwidth of 30 GHz are required to generate triangular or rectangular waveforms with repetition rate of 10 GHz. In order to generate high-speed RF waveforms, modulator and PD with higher bandwidths are required. Moreover, we can only control the power of the RF harmonics up to the third-order one. Thus, only the approximation of the desired waveform can be achieved, which reduces the flexibility of the proposed method to generate arbitrary waveforms.

References

[1] J. P. Yao, "Photonic generation of microwave arbitrary waveforms," *Opt. Comm.*, vol. 284, no. 15, pp. 3723–3736, Jul. 2011.
[2] Y. Park, M. H. Asghari, T.-J. Ahn, and J. Azaña, "Transform-limited picosecond pulse shaping based on temporal coherence synthesization," *Opt. Exp.*, vol. 15, no. 15, pp. 9584–9599, Jul. 2007.
[3] S. Boscolo, A. I. Latkin, and S. K. Turitsyn, "Passive nonlinear pulse shaping in normally dispersive fiber systems," *IEEE J. Quantum Electron.*, vol. 44, no. 12, pp. 1196–1203, Dec. 2008.
[4] A. I. Latkin, S. Boscolo, R. S. Bhamber, and S. K. Turitsyn, "Optical frequency conversion, pulse compression and signal copying using triangular pulses," in *Proc. 34th ECOC*, Brussels, Belgium, 2008, pp. 1–2.
[5] A. I. Latkin, S. Boscolo, R. S. Bhamber, and S. K. Turitsyn, "Doubling of optical signals using triangular pulses," *J. Opt. Soc. Amer. B*, vol. 26, no. 8, pp. 1492–1496, Aug. 2009.
[6] F. Parmigiani *et al.,* "Efficient optical wavelength conversion using triangular pulses generated using a superstructured fiber Bragg grating," presented at the Optical Fiber Communication Conf., San Diego, CA, USA, 2008, OMP3.
[7] F. Parmigiani *et al.,* "An efficient wavelength converter exploiting a grating-based saw-tooth pulse shaper," *IEEE Photon. Technol. Lett.*, vol. 20, no. 17, pp. 1461–1463, Sep. 2008.
[8] Z. Jiang, C.-B. Huang, D. E. Leaird, and A. M. Weiner, "Optical arbitrary waveform processing of more than 100 spectral comb lines," *Nature Photon.*, vol. 1, pp. 463–467, 2007.
[9] C. B. Huang, D. E. Leaird, and A. M. Weiner, "Time-multiplexed photonically enabled radio-frequency arbitrary waveform generation with 100 ps transitions," *Opt. Lett.*, vol. 32, no. 22, pp. 3242–3244, Nov. 2007.
[10] J. Ye *et al.,* "Photonic generation of triangular-shaped pulses based on frequency to time conversion," *Opt. Lett.*, vol. 36, no. 8, pp. 1458–1460, Apr. 2011.

[11] J. Li *et al.,* "Photonic-assisted periodic triangular-shaped pulses generation with tunable repetition rate," *IEEE Photon. Technol. Lett.*, vol. 25, no. 10, pp. 952–954, May 2013.
[12] J. Li *et al.,* "Performance analysis of a photonic-assisted periodic triangular-shaped pulses generator," *J. Lightw. Technol.*, vol. 30, no. 11, pp. 1617–1624, Jun. 2012.
[13] X. Liu *et al.,* "Photonic generation of triangular-shaped microwave pules using SBS-based optical carrier processing," *J. Lightw. Technol.* [Online]. Available: http://ieeexplore.ieee.org/xpls/abs_all.jsp?arnumber=6777536&tag=1
[14] J. Li *et al.,* "Photonic generation of triangular waveform signals by using a dual-parallel Mach–Zehnder modulator," *Opt. Lett.*, vol. 36, no. 19, pp. 3828–3830, Oct. 2011.
[15] F. Zhang, X. Ge, and S. Pan, "Triangular pulse generation using a dual-parallel Mach–Zehnder modulator driven by a single-frequency radio frequency signal," *Opt. Lett.*, vol. 38, no. 21, pp. 4491–4493, Nov. 2013.
[16] W. Liu and J. Yao, "Photonic generation of microwave waveforms based on a polarization modulator in a Sagnac loop," *J. Lightw. Technol.*, vol. 31, no. 10, pp. 1636–1644, May 2014.